Journal of Medicinal Chemistry

Article

Identification of an orally bioavailable chromene-based Selective Estrogen Receptor Degrader (SERD) that demonstrates robust activity in a model of tamoxifen-resistant breast cancer

Johnny Nagasawa, Steven Govek, Mehmet Kahraman, Andiliy Lai, Celine Bonnefous, Karensa Douglas, John Sensintaffar, Nhin Lu, Kyoungjin Lee, Anna Aparicio, Josh Kaufman, Jing Qian, Gang Shao, Rene Prudente, James D Joseph, Beatrice Darimond, Daniel Brigham, Kate Maheu, Richard Heyman, Peter Rix, Jeffrey H Hager, and Nicholas D. Smith

J. Med. Chem., **Just Accepted Manuscript** • DOI: 10.1021/acs.jmedchem.8b00921 • Publication Date (Web): 07 Aug 2018

ACS Publications

is published by the American Chemical Society. 1155 Sixteenth Street N.W., Washington, DC 20036

Identification of an orally bioavailable chromene-based Selective Estrogen Receptor Degrader (SERD) that demonstrates robust activity in a model of tamoxifen-resistant breast cancer

Johnny Nagasawa,[a] Steven Govek,[a] Mehmet Kahraman,[a] Andiliy Lai,[a] Celine Bonnefous,[a] Karensa Douglas,[a] John Sensintaffar,[b] Nhin Lu,[b] KyoungJin Lee,[c] Anna Aparicio,[c] Josh Kaufman,[c] Jing Qian,[b] Gang Shao,[b] Rene Prudente,[b] James D. Joseph,[b] Beatrice Darimont,[b] Daniel Brigham,[b] Kate Maheu,[b] Richard Heyman,[b] Peter J. Rix,[c] Jeffrey H. Hager,[b] Nicholas D. Smith[a]*

Seragon Pharmaceuticals, 12780 El Camino Real, Suite 302, San Diego, California 92130.

[a] Department of Chemistry, [b] Department of Biology, [c] Department of Drug Safety and Disposition

ABSTRACT About seventy-five percent of breast cancers are estrogen receptor alpha (ER-α) positive, and women typically initially respond well to anti-hormonal therapies such as tamoxifen and aromatase inhibitors, resistance often emerges. Fulvestrant is a steroid-based, selective estrogen receptor degrader (SERD) that both antagonizes and degrades ER-α, and shows some activity in patients who have progressed on anti-hormonal agents. However

fulvestrant must be administered by intra-muscular injections that limits its efficacy. We describe the optimization of ER-α degradation efficacy of a chromene series of ER modulators resulting in highly potent and efficacious SERDs such as **14n**. When examined in a xenograft model of tamoxifen-resistant breast cancer, **14n** (ER-α degradation efficacy = 91%) demonstrated robust activity, while despite superior oral exposure, **15g** (ER-α degradation efficacy = 82%) was essentially inactive. This result suggests that optimizing ER-α degradation efficacy in the MCF-7 cell line leads to compounds with robust effects in models of tamoxifen-resistant breast cancer derived from an MCF-7 back-ground.

KEYWORDS: Estrogen receptor, estrogen receptor degrader, SERD, antagonist, tamoxifen-resistant, breast cancer, chromene.

INTRODUCTION

The estrogen receptor ERα is a ligand-regulated transcription factor, and mediates the activity of estrogens in a number of physiological processes including reproduction, the cardiovascular system and bone density/remodeling.[1] The estrogen receptor (ER) is a well validated therapeutic target for a number of indications, and there are several ER ligands that are approved drugs for the treatment of cancer (tamoxifen, fulvestrant) and osteoporosis (raloxifene, bazodoxifene).[2] Tamoxifen (**1**) and its active metabolite, 4-hydroxytamoxifen (**2**) are selective estrogen receptor modulators (SERMs), in that they function as an antagonist or agonist depending on the tissue context.[1] Unfortunately, despite many women with breast cancer initially responding to tamoxifen, resistance often emerges.[3] ER has been shown to still play an active role in this resistant state,[4] and fulvestrant (**3**), a selective estrogen receptor degrader (SERD) that both antagonizes and induces degradation of ER-α, is of some clinical benefit in this patient

population.[5] However fulvestrant has poor pharmaceutical properties requiring delivery through an intra-muscular injection that limits the amount of drug that can be administered, and its maximal clinical response. We thus set out to identify SERD's where ER-α degradation efficacy was optimized prospectively, and which were orally bioavailable allowing robust, therapeutic levels of exposure to be achieved rapidly.

Figure 1: ER ligands

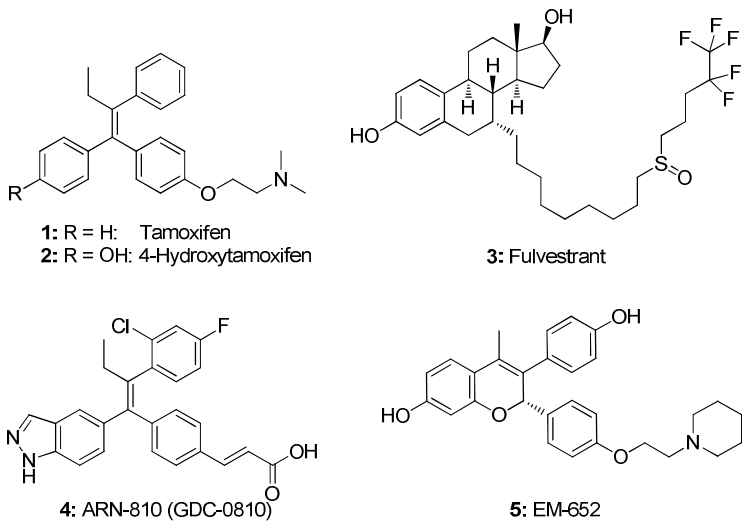

There is a wealth of information in the literature which provides an understanding of the structural elements required for high affinity ER ligand binding, but little has been described as to what is required for maximal ER-α degradation while maintaining antagonist activity (i.e. SERD activity). In order to prospectively optimize ER-α degradation, we utilized an in-cell western assay that monitored the levels of ER-α in MCF-7 breast cancer cells. This assay was key to defining the SAR of the program, including the identification of the clinical compound ARN-810/GDC-0810 (**4**) which was previously described (Figure 1).[6] This paper describes our

preliminary optimization of the chromene scaffold found in EM-652 (**5**, Figure 1),[7] ultimately leading to **14n**, a highly efficacious, orally bioavailable ER-α degrader with robust activity in a model of tamoxifen-resistant breast cancer.

Similar to the native ligand estradiol and many potent ER ligands in the literature, EM-652 has two free hydroxyls on its core structure, and these form key interactions in the ligand binding domain (LBD) of ER-α.[8] Appended to this core is a side-chain that is proposed to modulate the position of helix 12 of ER, and hence is the primary determinant of the antagonist/agonist properties of the ligand. Due to the presence of one or more phenols that can be readily glucuronidated in vivo, ER ligands typically suffer from low oral bioavailability and high clearance due to gut-wall and liver glucuronidation.[9] This is indeed the case with EM-652 which in our hands had low exposure following oral dosing in mice (AUC=0.09 μg·h/mL; 10 mg/kg peroral). However more recent work on related scaffolds had shown that the position of the phenol on the bicyclic core can have an unexpectedly dramatic effect on the PK properties. As shown in Figure 2 for dihydrobenzoxathiin[10] and chromane[11] scaffolds, the 6-OH phenol isomers have significantly higher rat oral bioavailability than the corresponding 7-OH phenol isomers (%F = 31 and 45, compared to %F = 0 and 2). In an attempt to maximize oral exposure, we applied this finding to the chromene scaffold and from the outset focused our SAR studies at maximizing ER-α degradation on a chromene core with a 6-OH.

Figure 2: Effect of phenol position on in-vivo clearance and bioavailability of dihydrobenzoxathiin and chromane scaffolds

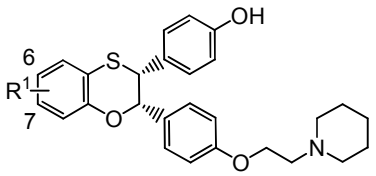

Dihydrobenzoxathiin scaffold:
R^1 = 6-OH: CL = 5 mL/min/Kg; %F = 31
R^1 = 7-OH: CL = 154 mL/min/Kg; %F = 0

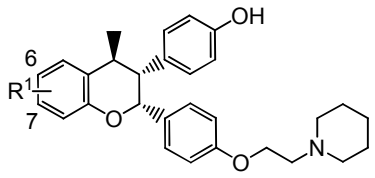

Chromane scaffold:
R^1 = 6-OH: CL = 7.7 mL/min/Kg; %F = 45
R^1 = 7-OH: CL = 9.5 mL/min/Kg; %F = 2

CHEMISTRY

The general strategy for the synthesis of new ER ligands was the coupling of an amino-alcohol side-chain (Scheme 1) and a central chromene core (Scheme 2) to produce the desired compounds (Schemes 2-4). Unsubstituted amino-alcohol side-chains **7b-d** were purchased from commercial sources, while **7a, 7e** and **7h** were prepared by alkylation of the appropriate cyclic amine with 2-bromoethanol (Scheme 1). The rest of the side-chains, all of which contained a stereo-center, were prepared by alkylation of an amino-alcohol with a bis-electrophile, so forming the cyclic amine structure. Thus **7f** and **7g** were prepared by reacting 2-aminoethanol with (*R*)- or (*S*)-2-methylbutane-1,4-diyl-dimethanesulfonate to give the pyrrolidine with the desired stereocenter on the ring. Compounds **7i, k-m**, with an (*S*)-methyl substituent on the chain were in turn prepared by alkylation of (*S*)-2-aminopropan-1-ol (**(*S*)-8**) with a di-halo alkane as shown. Similarly, alkylation of **(*S*)-8** or **(*R*)-8** with a bis-electrophile **9** containing a methyl substituent with either (*S*)- or (*R*)- stereochemistry, produced **7n-o** and **7j**, **7p**, **7q** respectively.

Scheme 1

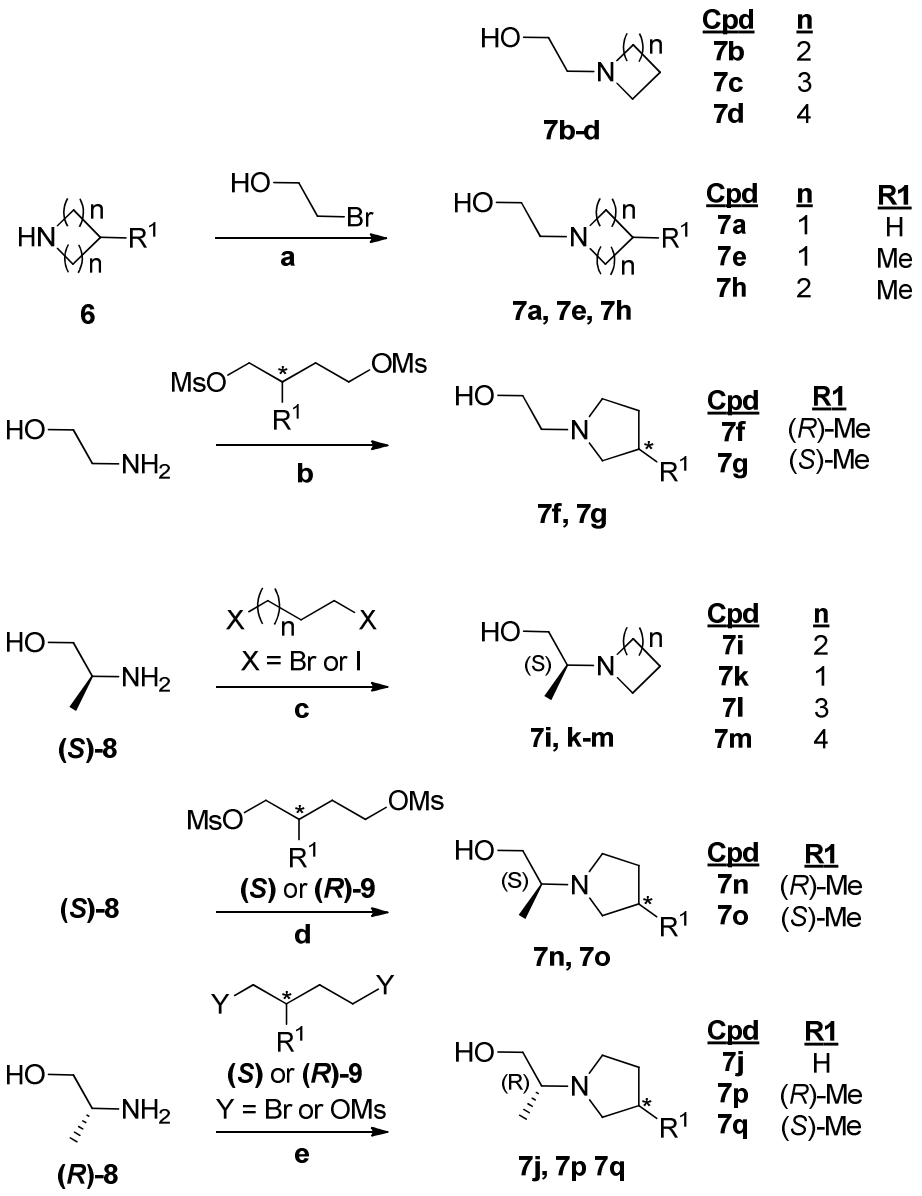

Reagents and conditions: (**a**) **7a**: Cs_2CO_3, acetonitrile, rt, 10%; **7e**: DBU, THF, rt, 73%; **7h**: TEA, $CHCl_3$, rt, 2 d, 21%; (**b**) **7f**: (*R*)-2-methylbutane-1,4-diyl dimethanesulfonate, K_2CO_3, acetonitrile, reflux, 20 h, 28%; **7g**: (*S*)-2-methylbutane-1,4-diyl dimethanesulfonate, K_2CO_3, acetonitrile. (**c**) **7i**: 1,4-dibromobutane, K_2CO_3, acetonitrile, reflux, on, 65%; **7k**: *i*) 1,3-dibromopropane, $NaHCO_3$, toluene, 130 °C, 22h *ii*) TBSCl, DMAP, TEA, toluene,rt, on, 13% (2 steps), *iii*) BF_3-OEt_2, $CHCl_3$/acetonitrile, rt, on, 69%; **7l**: 1,5-diiodopentane, Na_2CO_3, IPA, reflux, on, 54%; **7m**: 1,6-diiodohexane, Na_2CO_3, IPA, reflux, on, 60%. (**d**) **7n**: (*R*)-2-methylbutane-1,4-diyl dimethanesulfonate, neat, rt, on, 87%; **7o**: (*S*)-2-methylbutane-1,4-diyl dimethanesulfonate, K_2CO_3, acetonitrile, reflux. (**e**) **7j**: 1,4-dibromobutane, K_2CO_3, acetonitrile, 48%; **7p**: (*R*)-2-methylbutane-1,4-diyl dimethanesulfonate, K_2CO_3, acetonitrile, reflux; **7q**: (*S*)-2-methylbutane-1,4-diyl dimethanesulfonate, K_2CO_3, acetonitrile reflux.

Analogs **14a-q** were prepared from a common chromene intermediate **13a,** which was prepared in an eight step linear sequence as shown in Scheme 2. Starting material 2,5-dimethoxybenzoic acid (**10**) was converted to the Weinreb amide, and then treated with (3-methoxybenzyl)magnesium chloride to afford a tri-methoxy ketone intermediate. Demethylation with BBr_3 afforded **11** in 58% yield over the three steps. The 5 and 3' phenols of **11** were selectively protected with a THP group, and then cyclization with 4-iodobenzaldehyde gave THP-protected chromanone **12**. To install the double bond of the chromene, **12** was treated with methylmagnesium chloride to give the tertiary alcohol, followed by elimination to the alkene under acidic conditions using $AcOH/H_2O$. Under these elimination conditions deprotection of the THP groups also occurred, requiring re-protection to afford chromene **13a** in 56% over three steps. Finally, Ullmann coupling between **13a** and amino-alcohols **7a-q** in the presence of copper catalyst, followed by THP-deprotection using acetic acid, gave chromene analogs (**14a-q**) in 6-96% yield over 2 steps. The key Ullmann reaction was carried out in neat side-chain or at high concentration using butyronitrile or *m*-xylenes as a solvent, and in some cases, 2,2'bipyridine was used as a ligand.

Scheme 2

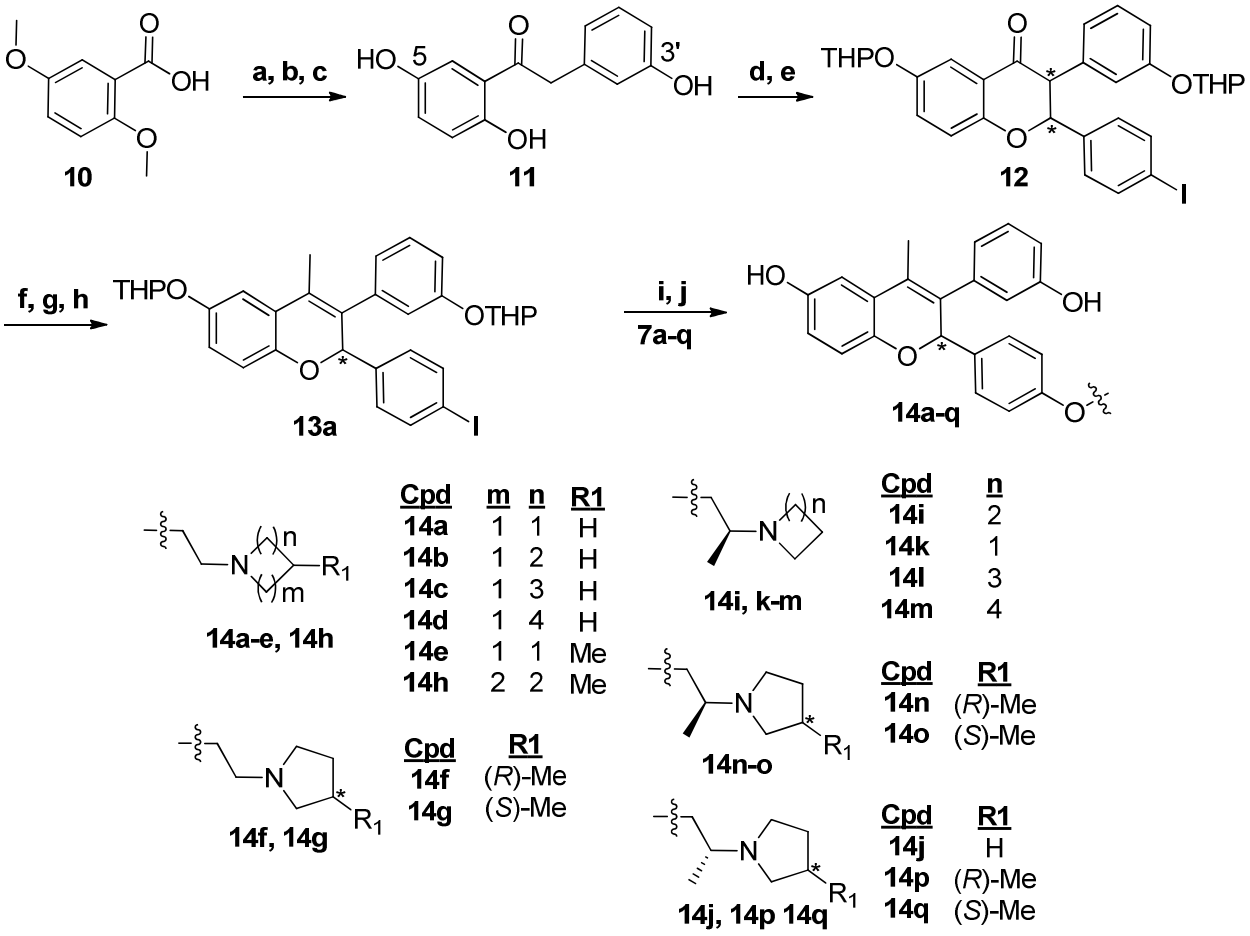

Cpd	m	n	R1
14a	1	1	H
14b	1	2	H
14c	1	3	H
14d	1	4	H
14e	1	1	Me
14h	2	2	Me

Cpd	n
14i	2
14k	1
14l	3
14m	4

Cpd	R1
14f	(*R*)-Me
14g	(*S*)-Me

Cpd	R1
14n	(*R*)-Me
14o	(*S*)-Me

Cpd	R1
14j	H
14p	(*R*)-Me
14q	(*S*)-Me

Reagents and conditions: (a) $(COCl)_2$, DMF, DCM, rt.; *N,O*-dimethylhydroxylamine hydrochloride, TEA, DCM, 0 ºC, 99%; (b) (3-methoxybenzyl)magnesium chloride, THF, 95%; (c) BBr_3, DCM, -78 ºC-0 ºC, 62%; (d) DHP, PPTS, DCM, 96%; (e) 4-iodobenzaldehyde, piperidine, DBU, *s*-butanol, reflux, 87%; (f) MeMgCl, THF, 0 ºC- rt.; (g) 80% AcOH/water, 90 ºC, 68% (2 steps); (h) DHP, PPTS, DCM, 95%; (i) For **14a-b**, **14d-e**, **14h**, **14j**, **14k, 14n**: CuI, K_2CO_3, (or Cs_2CO_3) butyronitrile, 125-135 °C, 2-4 d; for **14c**, **14f-i**, **14l-m**, **14o-q**: CuI, 2,2'-bipyridine, K_2CO_3, neat (or *m*-xylenes), 140 °C, on; (j) 80% AcOH/water, rt or 90 °C, 15 min (6-96% 2 steps).

As shown in Scheme 3, chromene phenol isomers **15b-d** were prepared by Ullman coupling of side-chain **7n** with iodochromene intermediates **13b-d** (which were prepared in an analogous way to that shown for **13a** in scheme 2), followed by acetic acid/water deprotection of the THP groups. In a similar way the monophenol analogues **15e-g** were prepared.

Scheme 3

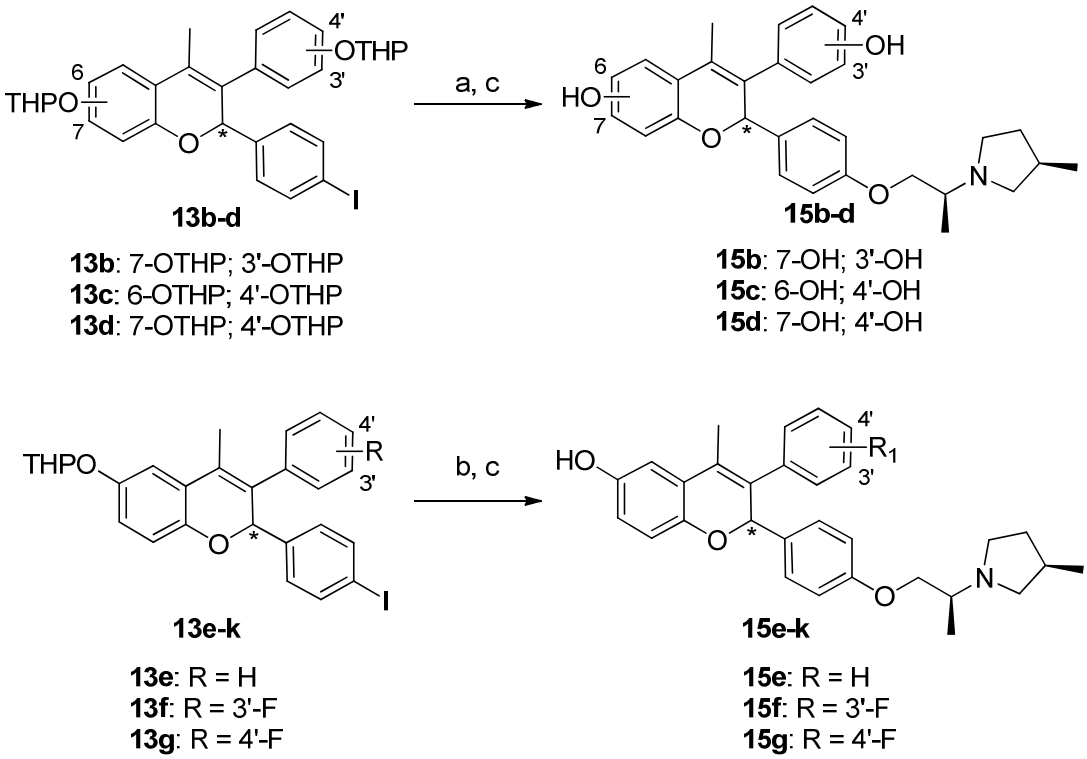

Reagents and conditions: (a) For **13b** and **13d**: **7n**, CuI, 2,2'-bipyridine, K_2CO_3, neat, 140 °C, o/n; for **13c**: **7n**, CuI, K_2CO_3, butyronitrile, 125-135 °C, 2-4 d; (b) **7n**, CuI, Cs_2CO_3 (or K_2CO_3) butyronitrile, 125-135 °C, 2-4 d; (c) 80% AcOH/water, rt or 90 °C, 15 min (37-65% 2 steps).

Other derivatives were prepared by palladium-catalyzed coupling with aryl halide intermediates as shown in scheme 4. Thus nitrile derivatives **15h-i** were prepared from the bromo or chlorophenyl intermediates **16h-i** using $Zn(CN)_2$ and [1,1'-binaphthalen]-2-yldi-*tert*-butylphosphine[12] followed by THP deprotection. In turn, **15j-k** were prepared from **16h-i** (R = Br) using sodium methanesulfinate and catalytic CuI/proline to install the sulfone group,[13] followed by THP deprotection.

Scheme 4

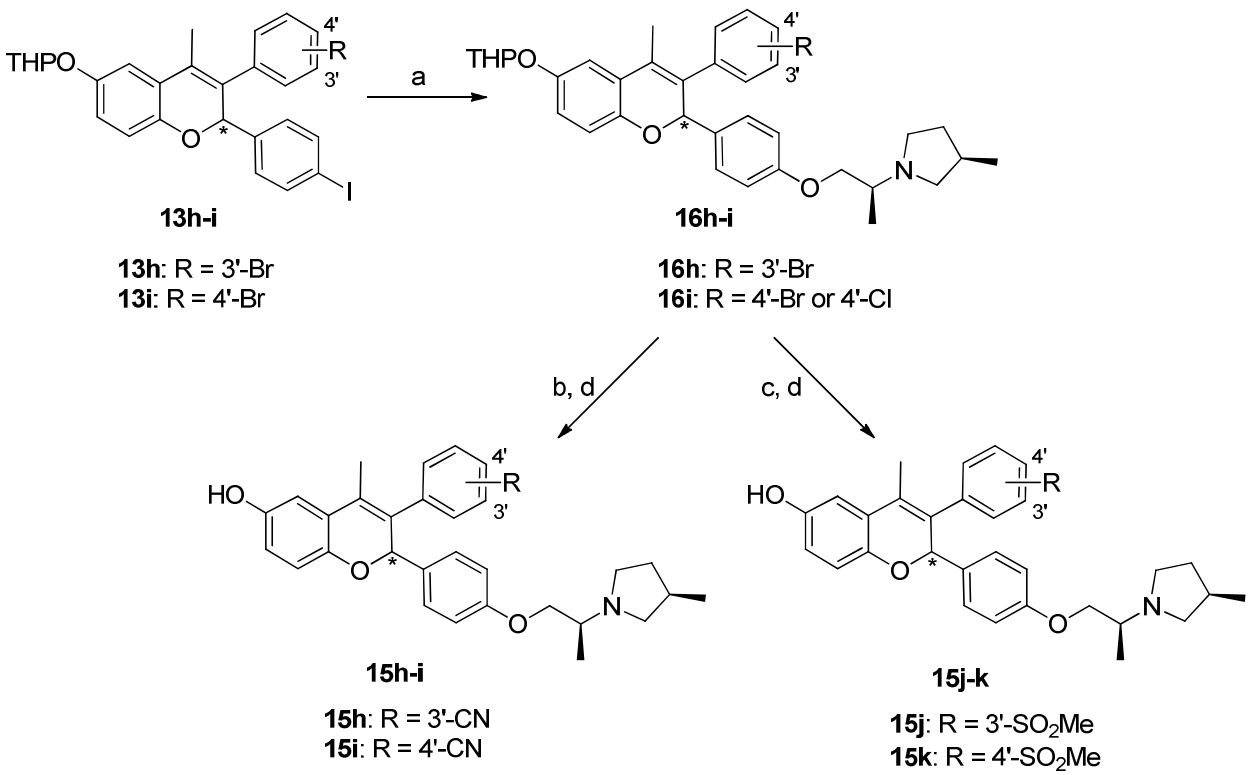

Reagents and conditions: (a) **7n**, CuI, K_2CO_3, butyronitrile, 135 °C, 2 d; (b) For **15h-i**: $Pd(TFA)_2$, $Zn(CN)_2$, Zn, [1,1'-binaphthalen]-2-yldi-*tert*-butylphosphine, DMA, 95 °C, 3.5h, 56%; (c) CuI, $MeSO_2Na$, *DL*-proline, NaOH, DMSO, 95 °C, on, 34%; (d) 80% AcOH/water, rt or 90 °C, 15 min (37-65%).

RESULTS AND DISCUSSION

Figure 3 shows the degree of ER-α degradation by 4-hydroxytamoxifen, fulvestrant and EM-652 as determined by the key in-cell western assay in MCF-7 cells. Fulvestrant was used as an internal control in each assay run, and we report degradation efficacy of compounds as a percent of this fulvestrant control. It should be noted that although potent, both 4-hydroxytamoxifen and EM-652 do not have the same level of ER-α degradation efficacy as fulvestrant. Despite being a

robust degrader, a small percentage of the ER-α still remains after fulvestrant treatment. This may reflect an inaccessible ER-α population resistant to degradation such as a nuclear insoluble fraction that is revealed upon cell permeabilization and antibody interrogation.[14]

Figure 3: MCF-7 ER-α degradation assay[a]

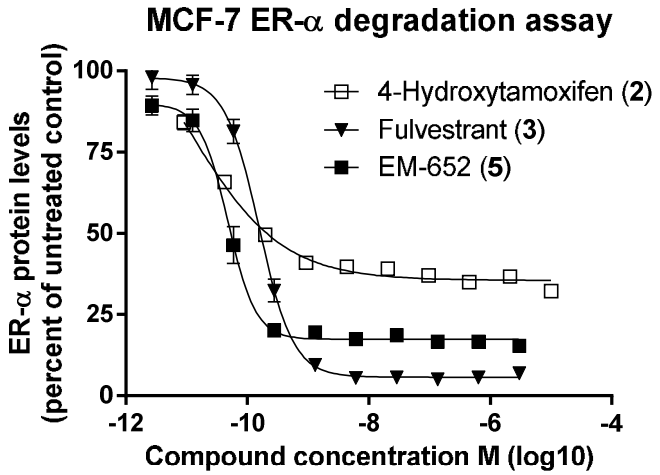

a: ER-α in-cell western in MCF-7 breast cancer cells in phenol-red free RPMI medium containing 5% charcoal dextran treated FBS; readings taken after 4 hours incubation using a SP-1 anti-ER rabbit monoclonal antibody

We initially examined the effect of ring size and alkyl substitution of the side-chain, in particular seeking to maximize ER-α degradation efficacy as monitored by the MCF-7 in-cell western assay. As shown in Table 1, all derivatives were potent ER-α degraders (IC_{50} < 1.0 nM) and had similar potency as antagonists of cell proliferation in the MCF-7 breast cancer cell line (IC_{50} < 0.5 nM). However the ER-α degradation efficacy varied depending on the ring size and substitution pattern of the side-chain. Of the unsubstituted nitrogen-containing heteroalkyl rings

of sizes from 4 to 7 (**14a-d**), piperidine **14c** had the highest degradation at 83% of the fulvestrant control. Interestingly, with methyl substitution on the ring (**14e-h**), an increase in degradation efficacy was obtained for azetidine **14e** (86%) and pyrrolidine **14f** (89%), while the piperidine derivative **14h** had a significant reduction in degradation efficacy (64%). Of note, the stereochemistry of the pyrrolidine methyl was important with the *(S)*-configuration isomer **14g** being an inferior degrader (77%) compared to the *(R)*-configuration isomer **14f** (89%). The importance of stereochemistry was also observed when substitution was examined on the linker, with *(S)*-methyl derivative **14i** being a good ER-α degrader (86%), while **14j**, with the opposite configuration was a poor degrader (58%). Whereas this (*S*)-configuration of the methyl on the linker increased degradation efficacy for **14i** over the parent pyrrolidine **14b** (86% versus 75%), installation of this methyl on the linker of other ring sizes, giving azetidine **14k**, piperidine **14l** or homopiperidine **14m**, did not lead to an increase in degradation efficacy over the unsubstituted parent compounds **14a**, **14c** or **14d**.

Table 1: Ring size and stereochemistry of methyl substitution of side-chain modulates degradation efficacy

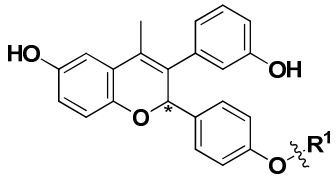

Compound	R^1	ER Degradation[a]		MCF-7 Proliferation[b]
		IC_{50} (nM)	Efficacy[c]	IC_{50} (nM)

14a	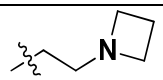	0.3	76	0.2
14b	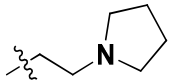	0.4	75	0.3
14c	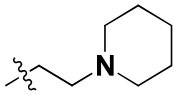	0.2	83	0.2
14d	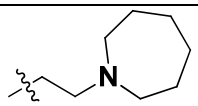	0.2	77	0.2
14e	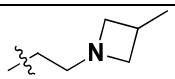	0.3	86	NT
14f	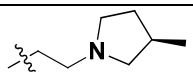	0.4	89	0.2
14g	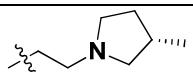	0.2	77	0.3
14h	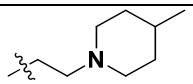	0.2	64	0.2
14i	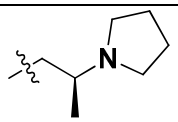	0.4	86	0.2
14j	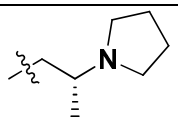	0.3	58	0.2
14k	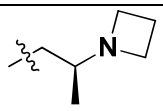	0.9	67	0.1

14l	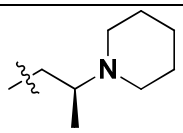	0.2	74	0.1
14m	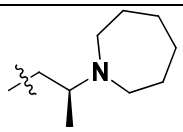	0.2	67	0.2
14n	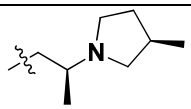	0.2	91	0.2
14o	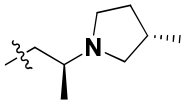	0.2	87	0.2
14p	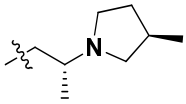	0.3	76	0.2
14q	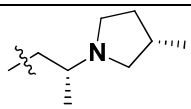	0.2	59	0.2

a: ER-α in-cell western in MCF-7 breast cancer cells in phenol-red free RPMI medium containing 5% charcoal dextran treated FBS; readings taken after 4 hours incubation using a SP-1 anti-ER rabbit monoclonal antibody ($n \geq 4$) b: MCF-7 proliferation assay in RPMI medium containing 10% FBS; 5 day incubation ($n \geq 3$) c: Efficacy recorded as percent of efficacy of fulvestrant control

Having identified substituted pyrrolidines **14f** and **14i** as compounds with increased ER-α degradation efficacy over the unsubstituted pyrrolidine, we combined both pieces of SAR (**14n**) and gained a further increase in ER-α degradation efficacy to 91% of the fulvestrant control. The importance of stereochemistry of the methyl substitution is again apparent as the stereoisomers **14o-q** are less effective degraders. Of further note is that for the pyrrolidine system, the linker

methyl is 'dominant' in driving ER degradation efficacy, as **14o** (87%) is more efficacious than **14p** (76%).

To maximize efficiency during our SAR studies, the compounds were prepared and tested in biological assays as a 1:1 mixture of stereosiomers at the chromene core. For key compounds in the program, we confirmed that ER-α binding and SERD activity lay in one isomer by separation and characterization of the stereoisomers. For example, the lead compound **14n** was separated by chiral supercritical fluid chromatography into two stereoisomers, **14na** and **14nb**. The active diastereoisomer **14na** had an ER-α binding IC_{50} = 2.8 nM, ER-α degradation IC_{50} = 0.1 nM and MCF-7 anti-proliferation IC_{50} = 0.1 nM. In contrast, diastereoisomer **14nb** was 50-100x less active in these assays, with this remaining activity likely due to residual **14na** in the sample (~ 1% remaining following separation of **14n**). Further, using a 3xERE transcription assay, we confirmed that **14nb** had no ER-α agonist properties, indicating that working with enantiomeric or diastereoisomeric mixtures was acceptable during SAR studies (that the ER activity resided in one chromene stereoisomer was confirmed for a number of pairs of compounds on the program).

Table 2: SERD activity resides in one chromene stereoisomer

Cpd	Structure	ER-α Binding	ER-α Degradation[a]		MCF-7 Proliferation[b]
		IC_{50} (nM)	IC_{50} (nM)	Efficacy[c]	IC_{50} (nM)
14n	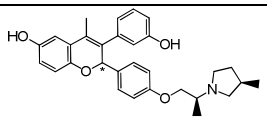	5.1	0.2	91	0.2

14na		2.8	0.1	91	0.1
14nb		136	9.7	90	59

a: ER-α in-cell western in MCF-7 breast cancer cells in phenol-red free RPMI medium containing 5% charcoal dextran treated FBS; readings taken after 4 hours incubation using a SP-1 anti-ER rabbit monoclonal antibody ($n \geq 4$) b: MCF-7 proliferation assay in RPMI medium containing 10% FBS; 5 day incubation ($n \geq 3$) c: Efficacy recorded as percent of efficacy of fulvestrant control

An *(S)*-stereochemistry at the chromene core of **14na** was unambiguously assigned by a single-crystal X-ray diffraction pattern of the (*R*)-mandelate salt (Figure 3).

Figure 3: Single-crystal X-ray structure of **14na**.mandalate salt confirms (*S*)-configuration at the chromene core

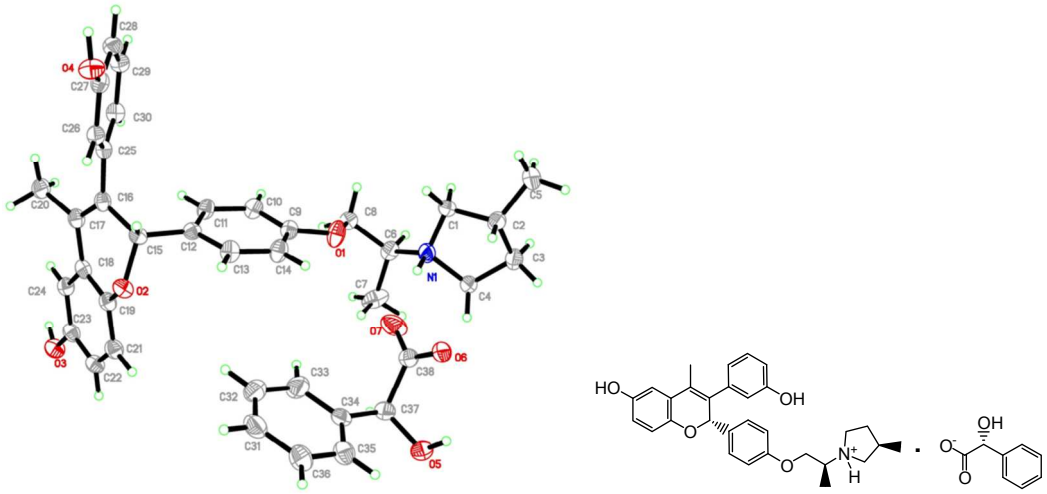

With the optimized chiral side-chain of **14n**, we examined the effect of the position of the two phenols of **14n** by preparing 3 regioisomers **15b**, **15c** and **15d** (Table 3). The in vitro profile of

these regioisomers were similar to that of **14n**, with all compounds demonstrating high potency and efficacy in the ER-α degradation assay (IC_{50} < 0.5 nM, efficacy >90%), and MCF-7 proliferation assay (IC_{50} < 0.3 nM). 6-OH Phenol **14n** was determined to be the preferred phenol configuration in terms of pharmacokinetics as it had 10-fold higher exposure following oral dosing in mice than its 7-OH phenol isomer **15b**. A similar trend was also observed when comparing the exposure of **15c** to **15d**.

Table 3:

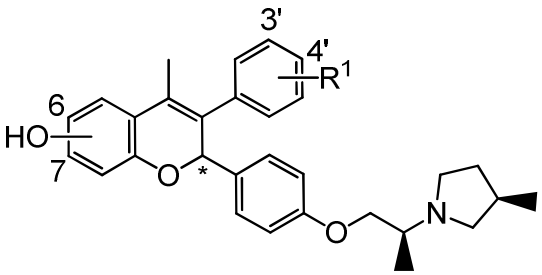

Cpd	Phenol	R[1]	ER Degradation[a]		MCF-7 Proliferation[b]	Mouse po Plasma AUC[15]
			IC_{50} (nM)	Efficacy[c]	IC_{50} (nM)	(μg·h/mL)
14n	6-OH	3'-OH	0.2	91	0.2	0.60
15b	7-OH	3'-OH	0.2	92	0.3	0.05
15c	6-OH	4'-OH	0.1	92	0.1	0.46
15d	7-OH	4'-OH	0.3	92	0.2	0.12
15e	6-OH	H	0.4	84	0.4	1.0
15f	6-OH	3'-F	0.5	88	1.0	0.35
15g	6-OH	4'-F	0.4	82	0.4	2.0

15h	6-OH	3'-CN	0.7	83	2.6	ND
15i	6-OH	4'-CN	1.5	84	10	2.0
15j	6-OH	3'-SO_2Me	1.4	73	4.3	ND
15k	6-OH	4'-SO_2Me	5.7	77	27	ND

a: ER-α in-cell western in MCF-7 breast cancer cells in phenol-red free RPMI medium containing 5% charcoal dextran treated FBS; readings taken after 4 hours incubation using a SP-1 anti-ER rabbit monoclonal antibody ($n \geq 4$) b: MCF-7 proliferation assay in RPMI medium containing 10% FBS; 5 day incubation ($n \geq 3$) c: Efficacy recorded as percent of efficacy of fulvestrant control

The major route of metabolism of **14n** is glucuronidation of one or both of the phenols, and so in an attempt to increase the oral exposure of the series, we examined replacement or removal of these metabolic liabilities. Indeed, removal of the 3'-OH of **15e**, led to an almost doubling in exposure over **14n** (**15e** mouse po AUC (10 mpk) = 1.0 μg·h/mL), and also retained ER-α degradation and MCF-7 proliferation potency. However, a pronounced reduction in ER-α degradation efficacy of **15e** compared to **14n** was observed (84% versus 91% respectively). Examination of a fluoro, cyano or methylsulfone group at the 3'- or 4'-positions of this ring (**15f-k**), did not lead to compounds with equivalent ER-α degradation to **14n**, but did indicate that lipophilic groups were preferred for potency in both the degradation and MCF-7 proliferation assays (compare: **15f** vs **15h** vs **15j** and **15g** vs **15i** vs **15k**). Of note, mono-phenols **15g** and **15i** displayed a further 3-fold improvement in oral exposure over **14n**. However **15i** was significantly less potent in the degradation and MCF-7 proliferation assays when compared to both **14n** and **15g**.

To rapidly assess ER-based pharmacodynamics in an ER responsive tissue, we utilized a 4-day immature rat uterine wet weight assay. The assay was run in two modalities, either in antagonist

mode where the test compound competes against ethynyl estradiol, or in agonist mode where no ethynyl estradiol was administered (revealing any inherent estrogenic activity of the ligand). Table 4 shows the reduction in ethynyl estradiol stimulated uterine weight (antagonist mode) for select compounds at either the SAR screening dose of 1 mg/kg or at a higher 10 mg/kg dose (the table also includes exposure from separate mouse PK studies). The 10 mg/kg dose was used to assess the maximum efficacy of the compound in this assay.

Table 4: Immature rat uterine wet weight assay (antagonist mode) and mouse pharmacokinetics

			Rat Uterine Wet Weight Assay[a]	**Mouse PK[c]**
Cpd	**ER Degradation IC_{50} (nM)**	**ER Degradation efficacy (%)**	**Reduction in uterine weight[b] (dose)**	**po AUC (μg·h/mL)**
Tamoxifen (1)	0.1[d]	51[d]	78% (60 mg/kg)	ND
Fulvestrant (3)	0.1	100	110% (200 mg/kg)	ND
14j	0.3	58	84% (10 mg/kg)	ND
14n	0.2	91	111%[e]	0.59

			(10 mg/kg)	
15c	0.1	92	113% (1 mg/kg)	0.46
15g	0.4	82	111% (1 mg/kg)	2.0

a: Compounds administered orally for 3 days (1 mg/kg po) followed by an oral dose of 0.1 mg/kg ethynyl estradiol. On the fourth day, 24 hours after dose, the animals were euthanized and the uterus was removed and weighed. Plasma was taken at the time point indicated. b: 100 x [($Vehicle_{EE}$ – Cpd)/($Vehicle_{EE}$ – Vehicle)], where '$Vehicle_{EE}$' is the uterine wet weight of the vehicle animals dosed with ethynyl estradiol (0.1 mg/kg); 'Cpd' is the uterine wet weight of the of the compound treated animals dosed with ethynyl estradiol (0.1 mg/kg); 'Vehicle' is the uterine wet weight of the of the vehicle animals. c: 10 mg/kg po. d: Values for 4-hydroxytamoxifen. e: At 1 mg/kg, reduction in uterine weight was 99%.

In this assay, **14n**, **15c** and **15g** were confirmed as compounds of interest as they had a robust reduction of >110% in uterine weight compared to the ethynyl estradiol treated vehicle animals, indicating they were inverse agonists in this ER-responsive tissue.[16] In contrast, tamoxifen (**1**) and **14j** did not reduce the uterine weight to that of ethynyl estradiol treated vehicle animals in this assay (78% and 84% reduction), and when run in agonist mode in the immature rat uterine wet weight assay, were shown to be partial agonists (figure 4). This partial agonist activity observed in the uterus (SERM activity) is well known for tamoxifen and is manifested both in preclinical models and in patients.[1] Of note, **14j** is a partial agonist, while the close structural analogue **14n** is an inverse agonist, reducing uterine wet weight below that of vehicle control. This divergent activity was also seen in the efficacy difference in the ER-α degradation assay (58% efficacy versus 91% respectively). High efficacy ER-α degraders were found to be robust

inverse agonists in the UWW assay throughout the program, although there is clearly a threshold as **15g**, which had sub-optimal ER-α degradation efficacy (82%), was a full antagonist in the uterine assay. Due to this and its improved exposure in mice (AUC = 2 μg.h/mL following a 10 mg/kg po dose), **15g** was selected for further profiling along with **14n**.

Figure 4: Tamoxifen (**1**) and **14j** are partial agonists in the immature rat uterine wet weight assay[a]

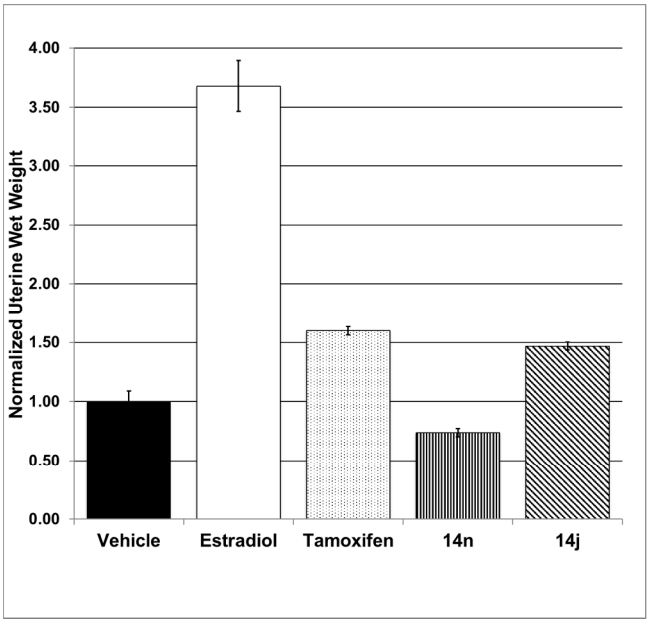

[a]: Compounds administered orally for 3 days (**14n** and **14j** at 10 mg/kg po; tamoxifen at 60 mg/kg). On the fourth day, 24 hours after dose, the animals were euthanized and the uterus was removed and weighed. Uterine wet weight is normalized to total body weight.

The full rat and mouse pharmacokinetic profiles for **14n** and **15g** are shown in Table 6. As would be expected mono-phenol **15g** has a lower clearance (CL = 21-30 mL/min/kg versus 33-38 mL/min/kg) and longer half-life ($t_{1/2}$ = 5-7 h versus 2-3 h) compared to bi-phenol **14n**, as well as

higher bioavailability (%F = 35-54 versus 13-18) and oral exposure (AUC = 2.0 – 4.5 versus 0.59 – 0.93 μg.h/mL).

Table 6: Rodent PK of **14n** and **15g**

Compound[a] **(Species)**	**CL (mL/min/kg)**	**V_{ss} (L/kg)**	**$t_{1/2}$ (h)**	**C_{max} (Oral) (μg/mL)**	**$AUC_{0\text{-}inf}$ (Oral) (μg·h/mL)**	**Oral %F**
14n (Mouse)	38	6.2	3.6	0.1	0.59	13
14n (Rat)	33	8.0	2.9	0.14	0.93	18
15g (Mouse)	30	11	5.2	0.17	2.0	35
15g (Rat)	21	12	7.4	0.28	4.5	54

a: Dosed intravenously at 3 mg/kg and per orally at 10 mg/kg in PEG400 / PVP / TW80 / 0.5% CMC in water, 9:0.5:0.5:90

14n and **15g** were profiled in MCF-7 based xenograft models of breast cancer using sub-cutaneous estradiol pellets to deliver sufficient levels of estradiol to drive tumor growth. This supplemental estradiol (E2) is used to drive xenograft tumor growth in vivo, and leads to high E2 concentrations (300-400 pg/mL), thus requiring more ER ligand to out-compete the native ligand

(E2) and so mediate an inhibitory effect. This is of relevance as plasma E2 levels in the target patient population of post-menopausal women (~5 pg/mL) are substantially lower than those of the various pre-clinical efficacy models.[17] Thus efficacy models run in the context of high E2 plasma concentrations potentially overestimate ER ligand dose and plasma levels necessary to drive efficacy in a post-menopausal setting. When examined in a MCF-7 tamoxifen-sensitive xenograft model, **14n** and **15g** (both dosed at 6mg/kg per orally QD), as well as tamoxifen (**1**) (60 mg/kg per orally QD) showed robust activity even in this high estradiol setting (Figure 5).

Figure 5: 14n and **15g** show robust activity in a tamoxifen-sensitive MCF-7 xenograft model

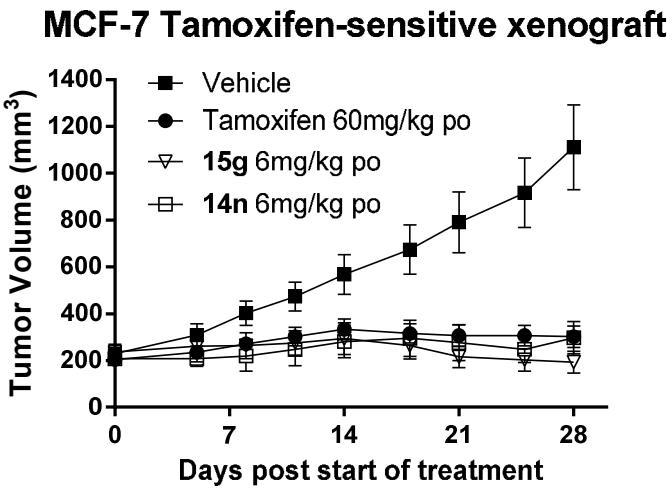

As the target patient population for SERDs is women who have progressed on endocrine therapy, including tamoxifen, we developed models of endocrine resistance by continuous dosing of tamoxifen to mice bearing MCF-7 xenograft tumors until re-growth occurred. These individual tumors that were resistant to tamoxifen were then propagated under chronic tamoxifen dosing and used as the source material for tamoxifen-resistant xenograft studies. The activity of **14n** and

15g in one such model is shown in Figure 6, and an interesting divergence of activities was observed.

Figure 6: Optimized ER-α degrader **14n** demonstrated tumor stasis in an MCF-7 tamoxifen-resistant xenograft model

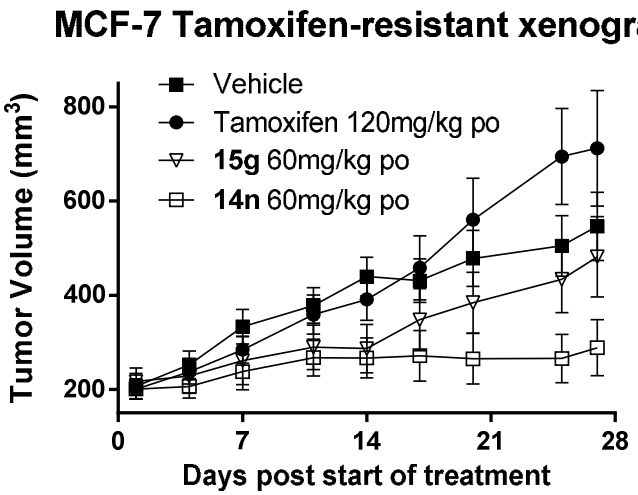

Encouragingly**, 14n** was active in this tamoxifen-resistant model giving tumor stasis at 60 mg/Kg. In contrast to the tamoxifen-sensitive xenograft (figure 5), **15g** had minimal activity, effectively growing like vehicle control. The inferior profile of **15g** compared to **14n** is not due to potency against the estrogen receptor (ER-α degradation IC_{50}: **15g** = 0.4 nM, versus **14n** = 0.2 nM; MCF-7 proliferation IC_{50}: **15g** = 0.4 nM versus **14n** = 0.2 nM) or pharmacokinetics (day 28 xenograft AUC: **14n** = 4.6 μg·h/mL; **15g** = 36 μg·h/mL). Of note however, is **15g** is a less efficacious ER-α degrader than **14n** in vitro (ER-α degradation efficacy = 82% versus 91%). This is consistent with our previous conclusion that compounds with lower ER-α degradation efficacy did not perform as well in a tamoxifen-resistant xenograft setting.[6]

In summary, we have optimized ER-α degradation efficacy on a chromene series of estrogen receptor modulators resulting in highly potent and efficacious SERDs. Side-chain ring size and stereochemical elements were central in driving degradation efficacy, leading to the identification of **14n**. SAR studies revealed that potency could be maintained and pharmacokinetic parameters improved when one of the two phenol moieties was removed, but this resulted in a significant erosion in degradation efficacy. In a xenograft model of tamoxifen-resistant breast cancer, **14n** (ER-α degradation efficacy = 91%) demonstrated robust activity, while despite superior oral exposure, mono-phenol **15g** (ER-α degradation efficacy = 82%) was essentially inactive. This result suggests that optimizing ER-α degradation efficacy in the MCF-7 cell line leads to compounds with robust effects in models of tamoxifen-resistant breast cancer derived from an MCF-7 back-ground.

EXPERIMENTAL SECTION

Experimental Procedures (Chemistry)

All air and moisture sensitive reactions were carried out under an inert atmosphere of nitrogen. All reactive liquid reagents were transferred by syringe or cannula and were added into the flask through a rubber septum. All other solvents and reagents were obtained from commercial sources and used as received unless otherwise stated. Both ^{1}H and ^{13}C spectra were obtained on a Bruker 400 spectrometer at 400 MHz and 100 MHz, respectively. Chemical shifts are reported in parts per million (δ) from an internal standard of residual DMSO (2.50 ppm or 39.5 ppm), methanol (3.31 ppm or 49.0 ppm), or chloroform (7.26 ppm or 77.2 ppm). Proton chemical shift data are reported as follows: chemical shift, multiplicity (s=singlet, d=doublet, t = triplet, q = quartet, m = multiplet, b = broad), coupling constant (*J*) reported in hertz, integration. Analytical

thin-layer chromatography (TLC) was performed on commercial silica plates (Merck 60-F 254, 0.25 mm thickness); compounds were visualized by UV light (254 nm). All yields reported are not optimized. Normal phase purifications were performed on silica gel columns using a Biotage (SP1 or SP4), an ISCO Combiflash Companion XL or ISCO Combiflash Torrent using pre-packed silica gel columns. Reversed phase semipreparative HPLC purifications were carried out using a Shimadzu Discovery VP system with a SPD-20A prominence UV/vis detector (190-700 nm range). The columns used were a Waters SunFire C18 (19 mm x 150 mm) or a YMC-Pack Pro ODS-A (20 mm x 150 mm) or a Phenomenex, Luna 5 μ C18 semipreparative (250 x 10 mm) column with an acetonitrile-water solvent mixture in the presence of 0.1% TFA. The purity of target compounds was determined by ^{1}H NMR and by analytical HPLC and shown to be > 95% pure prior to biological testing. Low-resolution mass spectra (LRMS) were recorded on a WatersMicromass ZQ using electrospray positive ionization. High-resolution mass spectra (HRMS) were obtained on an Agilent ESI-TOF mass spectrometer using electrospray positive or negative ionization.

For full experimental details of all compounds, see Supplementary Information

(R)-2-Methylbutane-1,4-diyl dimethanesulfonate. Triethylamine (100 mL, 0.72 mol) was added to a solution of (*R*)-2-methylbutane-1,4-diol (30 g, 0.29 mol) in DCM (600 mL) at room temperature. The solution was cooled to -20 °C, and methanesulfonyl chloride (49 mL, 0.63 mol) was added dropwise over 30 min with vigorous stirring. The resulting mixture was stirred for additional 1 h while the temperature was maintained between -20 and -15 °C. The mixture was allowed to warm to 0 °C and then poured into cold 1N HCl solution (100 mL). The organic layer was separated, and the aqueous phase was extracted with DCM (100 mL). The combined organic

extracts were washed (saturated $NaHCO_3$ and then brine), dried ($MgSO_4$), and concentrated *in vacuo*. The resulting product (75.9 g, quant) was used directly for the next step. ^{1}H NMR (400 MHz, DMSO-d_6): δ 4.32-4.22 (m, 2H), 4.13-4.03 (m, 2H), 3.18 (s, 2 x 3H), 2.02-1.92 (m, 1H), 1.87-1.77 (m, 1H), 1.61-1.50 (m, 1H), 1.07 (d, J = 6.8 Hz, 3H).

(S)-2-((R)-3-Methylpyrrolidin-1-yl)propan-1-ol. (*R*)-2-Methylbutane-1,4-diyl dimethanesulfonate (37.5 g, 0.144 mol,) was added to neat (*S*)-2-aminopropan-1-ol (54.8 g, 0.730 mol) at room temperature. The mixture was stirred in a room temperature water bath to minimize the exotherm. After 24 h, the reaction was diluted with DCM (150 mL), saturated K_2CO_3 solution (150 mL), and just enough water (60 mL) to dissolve the resulting precipitate. The layers were separated, and the aqueous layer was extracted with DCM (150 mL). The organic layers were combined, dried (Na_2SO_4), concentrated, and purified by silica gel chromatography (10: 7; ethyl acetate: hexanes → 10: 7: 2: 1; ethyl acetate: hexanes: methanol: triethylamine) to give the title compound (17.9 g, 87%) as a pale yellow oil. ^{1}H NMR (400 MHz, DMSO-d_6): δ 4.33 (t, J = 5.4 Hz, 1H), 3.51-3.43 (m, 1H), 3.21-3.13 (m, 1H), 2.79 (dd, J = 8.6, 7.6 Hz, 1H), 2.62-2.54 (m, 1H), 2.51-2.43 (m, 1H), 2.30-2.20 (m, 1H), 2.15-2.03 (m, 1H), 2.01 (dd, J = 8.6, 6.8 Hz, 1H), 1.91-1.81 (m, 1H), 1.25-1.15 (m, 1H), 0.98 (d, J = 6.4 Hz, 3H), 0.96 (d, J = 6.5 Hz, 3H); ^{13}C NMR (100 MHz, DMSO-d_6): δ 64.5, 60.1, 58.8, 50.4, 32.0, 31.1, 20.3, 12.2; LCMS: 144.3 $[M+H]^+$.

2-(4-Iodophenyl)-4-methyl-6-((tetrahydro-2H-pyran-2-yl)oxy)-3-(3-((tetrahydro-2H-pyran-2-yl)oxy)phenyl)-2H-chromene (13a)

Step 1: N,2,5-Trimethoxy-N-methylbenzamide. Oxalyl chloride (3.6 mL, 41.3 mmol) was added to a solution of 2,5-dimethoxybenzoic acid (**10**) (6.00 g, 33.0 mmol) in DCM (100 mL) at room temperature. Then, DMF (0.2 mL) was added to the solution. The resulting solution was stirred at room temperature for 2 h, and the solvent was removed on a rotary evaporator. The crude material was placed under vacuum for 30 minutes (to remove the residual oxalyl chloride), dissolved in DCM (100 mL), and cooled to 0 °C. To this solution, *N,O*-dimethylhydroxylamine hydrochloride (4.03 g, 41.32 mmol) and triethylamine (6.8 mL, 48.78 mmol) were added. The resulting mixture was stirred at 0 °C for 30 min and then at room temperature for additional 30 min. The reaction was diluted with DCM (50 mL), washed (2×100 mL water and then 100 mL brine), dried (Na_2SO_4), and concentrated under reduced pressure. The crude material was purified by silica gel chromatography to yield the title compound (7.32 g, 99%) as clear oil which solidified over time. ^{1}H NMR (400 MHz, $CDCl_3$): δ 6.95-6.84 (m, 3H), 3.82 (s, 3H), 3.79 (s, 3H), 3.58 (br, 3H), 3.32 (br, 3H).

Step 2: 1-(2,5-Dimethoxyphenyl)-2-(3-methoxyphenyl)ethanone. A 5 mL portion of 3-methoxybenzyl chloride (12.8 mL, 88.1 mmol) in THF (60 mL) was added to a mixture of magnesium (2.88 g, 118 mmol) and iodine (1 crystal) in THF (30 mL) at room temperature. The reaction mixture was stirred until the color disappeared and the remaining solution of 3-methoxybenzyl chloride was added dropwise over 45 min. The mixture was heated at 60 °C for 1 h and then cooled to 0 °C. A solution of *N*,2,5-trimethoxy-*N*-methylbenzamide (6.65 g, 29.6 mmol) in THF (70 mL) was added to this mixture over 30 min at 0 °C. The reaction was stirred for 30 min at 0 °C, quenched with brine (50 mL), and then extracted with ethyl acetate (3×100 mL). The combined organic extracts were washed (50 mL brine), dried (Na_2SO_4), and concentrated under reduced pressure to give the title compound (7.99 g, 95%) as a white solid.

^{1}H NMR (400 MHz, $CDCl_3$): δ 7.27-7.20 (m, 2H), 7.01 (dd, *J* = 9.0, 3.2 Hz, 1H), 6.92 (d, *J* = 9.0 Hz, 1H), 6.86-6.76 (m, 3H), 4.30 (s, 2H), 3.90 (s, 3H), 3.82 (s, 3H), 3.79 (s, 3H).

Step 3: 1-(2,5-Dihydroxyphenyl)-2-(3-hydroxyphenyl)ethanone. Boron tribromide (1M in DCM, 48.0 mL, 48.0 mmol) was added dropwise to a solution of 1-(2,5-dimethoxyphenyl)-2-(3-methoxyphenyl)ethanone (3.35 g, 11.7 mmol) in DCM (50 mL) at -78 °C. The reaction mixture was warmed to 0 °C, stirred for 30 min, re-cooled to -78 °C, and then quenched with methanol (15 mL). The reaction mixture was warmed to room temperature, concentrated under reduced pressure, and purified by silica gel chromatography to give the title compound (1.78 g, 62%) as a yellow solid. ^{1}H NMR (400 MHz, DMSO-d_6): δ 11.24 (s, 1H), 9.34 (s, 1H), 9.20 (s, 1H), 7.26 (d, *J* = 3.0 Hz, 1H), 7.10 (t, *J* = 7.8 Hz, 1H), 6.98 (dd, *J* = 8.9, 3.0 Hz, 1H), 6.83 (d, *J* = 8.9 Hz, 1H), 6.70-6.58 (m, 3H), 4.24 (s, 2H); LCMS: 243.0 $[M-H]^-$.

Step 4: 1-(2-Hydroxy-5-((tetrahydro-2H-pyran-2-yl)oxy)phenyl)-2-(3-((tetrahydro-2H-pyran-2-yl)oxy)phenyl)ethanone. A solution of 3,4-dihydro-2*H*-pyran (2.65 g, 30.8 mmol) in DCM (6 mL) was added to a mixture of **11** (1.50 g, 6.15 mmol) and pyridinium *p*-toluenesulfonate (320 mg, 1.27 mmol) in DCM (40 mL) at room temperature. The reaction mixture was stirred for 1 h and then diluted with DCM (100 mL). The solution was washed (2×50 mL saturated $NaHCO_3$ and then 50 mL brine), dried (Na_2SO_4), and concentrated under reduced pressure. The crude material was purified by silica gel chromatography to give the title compound (2.42 g, 96%) as yellow oil which solidified over time. ^{1}H NMR (400 MHz, $CDCl_3$): δ 11.88 (s, 1H), 7.63-7.56 (m, 1H), 7.31-7.20 (m, 2H), 7.03-6.96 (m, 2H), 6.94-6.92 (m, 2H), 5.46-5.40 (m, 1H), 5.31-5.25 (m, 1H), 4.25 (s, 2H), 4.00-3.86 (m, 2H), 3.70-3.52 (m, 2H), 2.07-1.55 (m, 12H); LCMS: 413.2 $[M+H]^+$.

Step 5: 2-(4-Iodophenyl)-6-((tetrahydro-2H-pyran-2-yl)oxy)-3-(3-((tetrahydro-2H-pyran-2-yl)oxy)phenyl)chroman-4-one. A solution of 1-(2-hydroxy-5-((tetrahydro-2*H*-pyran-2-yl)oxy)phenyl)-2-(3-((tetrahydro-2*H*-pyran-2-yl)oxy)phenyl)ethanone (2.41 g, 5.84 mmol), 4-iodobenzaldehyde (1.37 g, 5.91 mmol), piperidine (166 mg, 1.95 mmol), and 1,8-diazabicyclo[5.4.0]undec-7-ene (301 mg, 1.98 mmol) in *s*-butanol (10 mL) was heated at reflux. Using a Dean-Stark trap, half (5 mL) of the solvent was collected over 45 min, and the reaction was kept at reflux without further concentration for additional 45 min. The reaction mixture was cooled to 90 °C, 2-propanol (10 mL) was added, and the reaction was allowed to cool to room temperature and then stirred overnight. The resulting precipitate was collected by filtration to yield the title compound (3.17 g, 87%) as a white solid. ^{1}H NMR (400 MHz, DMSO-d_6): δ 7.63 (d, J = 8.3 Hz, 2H), 7.42 (t, J = 3.0 Hz, 1H), 7.36-7.28 (m, 1H), 7.23-7.15 (m, 2H), 7.14-7.04 (m, 2H), 6.80-6.69 (m, 3H), 5.93-5.81 (m, 1H), 5.50-5.43 (m, 1H), 5.37-5.28 (m, 1H), 4.60 (d, J = 12.3 Hz, 1H), 3.80-3.40 (m, 4H), 1.90-1.55 (m, 12H).

Step 6: 3-(3-Hydroxyphenyl)-2-(4-iodophenyl)-4-methyl-2H-chromen-6-ol. Methyl magnesium chloride (3M in THF, 4.0 mL, 12 mmol) was added dropwise to a solution of **12** (1.99 g, 3.18 mmol) in THF (40 mL) at 0 °C. The reaction was stirred at 0 °C for 15 min and then allowed to warm to room temperature. After stirring for 2 h, the solution was cooled to 0 °C, quenched with saturated ammonium chloride, and then allowed to warm to room temperature. Ethyl acetate (100 mL) and water (50 mL) were added, and the layers were separated. The organic layer was dried (Na_2SO_4), concentrated under reduced pressure, and purified by silica gel chromatography to yield a white foam (1.75 g). A solution of this purified material in 80% acetic acid/water (50 mL) was heated at 90 °C overnight. The solution was diluted with ethyl acetate (100 mL), washed (50 mL water, 50 mL saturated $NaHCO_3$ and then

50 mL brine), dried (Na_2SO_4), and concentrated under reduced pressure. The crude material was purified by silica gel chromatography to give the title compound (0.99 g, 68%) as a beige solid. ^{1}H NMR (400 MHz, DMSO-d_6): δ 9.46 (s, 1H), 9.00 (s, 1H), 7.62 (d, J = 8.3 Hz, 2H), 7.17 (t, J = 8.0 Hz, 1H), 7.01 (d, J = 8.3 Hz, 2H), 6.77-6.60 (m, 4H), 6.51 (s, 2H), 5.90 (s, 1H), 2.03 (s, 3H); LCMS: 455.0 $[M-H]^-$.

3-(4-Fluorophenyl)-2-(4-iodophenyl)-4-methyl-6-((tetrahydro-2H-pyran-2-yl)oxy)-2H-chromene (13g)

Step 1: 1-(2,5-Dimethoxyphenyl)-2-(4-fluorophenyl)ethanone. Polyphosphoric acid (330 g) was heated at 75 °C for 4.5 h, and then 1,4-dimethoxybenzene (48.0 g, 347 mmol) and 4-fluorophenyl acetic acid (30.1 g, 195 mmol) were added. The reaction was mixed thoroughly with a spatula until homogenous, heated at 75 °C for 17 h, allowed to cool to 50 °C, and then quenched by portion-wise addition of water (160 mL) while stirring with a spatula. The mixture was cooled to room temperature with an ice water bath, diluted with ice water (160 mL), and then extracted with ethyl acetate (1×400 mL, 2×200 mL). The combined organic extracts were washed with brine (300 mL), dried (Mg_2SO_4), concentrated under reduced pressure, and purified by silica gel chromatography (0–10% ethyl acetate in hexanes) to give the title compound (18.9 g, 35%) as a pink solid. ^{1}H NMR (400 MHz, DMSO-d_6): δ 7.27-7.20 (m, 2H), 7.15-7.07 (m, 5H), 4.26 (s, 2H), 3.85 (s, 3H), 3.72 (s, 3H).

Step 2: 1-(2,5-Dihydroxyphenyl)-2-(4-fluorophenyl)ethanone. A solution of 1-(2,5-dimethoxyphenyl)-2-(4-fluorophenyl)ethanone (18.9 g, 68.9 mmol) and DCM (275mL) at -78 °C was degassed with three vacuum/N_2 cycles. Boron tribromide (20.0 mL, 208 mmol) was added dropwise over 40 min. The reaction was stirred at -78 °C for 20 min, stirred at 0 °C for 40 min,

re-cooled to -78 °C, and then quenched by dropwise addition of methanol (35 mL) over 55 min. The mixture was diluted with ice water (400 mL), ethyl acetate (150 mL), and then additional water (200 mL). The layers were partitioned, and the organic extract was washed (400 mL $NaHCO_3$ and then 400 mL brine), dried ($MgSO_4$), and concentrated under reduced pressure to give the title compound (17.1 g, quant). ^{1}H NMR (400 MHz, DMSO-d_6): δ 11.12 (s, 1H), 9.22 (s, 1H), 7.33-7.26 (m, 3H), 7.19-7.11 (m, 2H), 7.03-6.93 (m, 1H), 6.82 (d, J = 8.9 Hz, 1H), 4.23 (s, 2H).

Step 3: 2-(4-Fluorophenyl)-1-(2-hydroxy-5-((tetrahydro-2H-pyran-2-yl) oxy)phenyl) ethanone. Pyridinium *p*-toluenesulfonate (3.50 g, 13.9 mmol) and 3,4-dihydro-2*H*-pyran (19.0 mL, 208 mmol) were added to a mixture of 1-(2,5-dihydroxyphenyl)-2-(4-fluorophenyl)ethanone (17.2 g, 69.6 mmol) and DCM (345 mL) at room temperature. After stirring for 2.5 h, the solution was washed (400 mL $NaHCO_3$). The aqueous layer was back extracted with DCM (100 mL). The combined organic layers were dried ($MgSO_4$), concentrated under reduced pressure, and purified by silica gel chromatography (0–10% ethyl acetate in hexanes) to give the title compound (18.8 g, 81%) as a yellow/pink solid. ^{1}H NMR (400 MHz, DMSO-d_6): δ 11.31 (s, 1H), 7.58 (d, J = 3.1 Hz, 1H), 7.33-7.27 (m, 2H), 7.25 (dd, J = 8.9, 3.0 Hz, 1H), 7.15 (m, 2H), 6.92 (d, J = 8.9 Hz, 1H), 5.44-5.38 (m, 1H), 4.49-4.38 (m, 2H), 3.83-3.75 (m, 1H), 3.58-3.50 (m, 1H), 1.94-1.68 (m, 3H), 1.68-1.48 (m, 3H); LCMS: 329 $[M-H]^-$.

Step 4: 3-(4-Fluorophenyl)-2-(4-iodophenyl)-6-((tetrahydro-2H-pyran-2-yl)oxy)chroman-4-one. Piperidine (4.0 mL, 40 mmol) and 1,8-diazabicyclo[5.4.0]undec-7-ene (6.0 mL, 40 mmol) were added to a mixture of 2-(4-fluorophenyl)-1-(2-hydroxy-5-((tetrahydro-2*H*-pyran-2-yl)oxy)phenyl)ethanone (40.5 g, 123 mmol), 4-iodobenzaldehyde (28.5 g, 123 mmol), and *s*-

butanol (130 mL) at room temperature. The reaction was heated at 135 °C, and solvent (~42 mL) was removed *via* Dean-Stark trap over 2 h [Note: product started to precipitate after removing ~30 mL of solvent]. The reaction was allowed to cool to 80 °C, 2-propanol (130 mL) was added, and then the reaction was allowed to cool to room temperature. After stirring for 3 days, the precipitate was collected by filtration to give the title compound (63.8 g, 95%) as a white solid. ^{1}H NMR (400 MHz, DMSO-d_6): δ 7.64 (d, J = 8.0 Hz, 2H), 7.44-7.40 (m, 1H), 7.36-7.29 (m, 1H), 7.21-7.10 (m, 4H), 7.07 (d, J = 8.9 Hz, 1H), 7.02 (t, J = 8.8 Hz, 2H), 5.89 (dd, J = 12.5, 1.9 Hz, 1H), 5.50-5.43 (m, 1H), 4.71 (d, J = 12.5 Hz, 1H), 3.79-3.70 (m, 1H), 3.59-3.50 (m, 1H), 1.93-1.69 (m, 3H), 1.69-1.48 (m, 3H); LCMS: 545 $[M+H]^+$.

Step 5: 3-(4-Fluorophenyl)-2-(4-iodophenyl)-4-methyl-2H-chromen-6-ol. Methylmagnesium chloride (3M in THF, 120 mL, 360 mmol) was added dropwise over 2 h to a mixture of 3-(4-fluorophenyl)-2-(4-iodophenyl)-6-((tetrahydro-2*H*-pyran-2-yl)oxy)chroman-4-one (63.8 g, 117 mmol) and THF (330 mL) at 0 °C. The reaction was stirred at 0 °C for 40 min and then allowed to warm to room temperature. After stirring for an additional 1.75 h, the reaction was cooled to 0 °C, quenched by dropwise addition of saturated ammonium chloride (100 mL), and then diluted with ethyl acetate (600 mL) and water (700 mL). The layers were separated, and the organic layer was washed (500 mL brine, 500 mL water, and then the first brine wash), dried ($MgSO_4$), concentrated under reduced pressure, and then dried under high vacuum. The crude material was triturated with dichloromethane to give a white solid. A solution of this solid in acetic acid/water (4: 1; 400 mL) was heated at 100 °C for 4 days, cooled to room temperature, concentrated, and then diluted with ethyl acetate (400 mL). This solution was washed (2×300 mL $NaHCO_3$, 200 mL water and then 200 mL brine), dried ($MgSO_4$), concentrated under reduced pressure, and then purified by silica gel chromatography (0–15% ethyl acetate in hexanes) to give the title

compound (41.1 g, 77%) as a pink solid. ^{1}H NMR (400 MHz, DMSO-d_6): δ 9.02 (s, 1H), 7.60 (d, J = 8.3 Hz, 2H), 7.37-7.31 (m, 2H), 7.18 (t, J = 8.9 Hz, 2H), 7.08 (d, J = 8.6 Hz, 2H), 6.76 (s, 1H), 6.55-6.50 (m, 2H), 5.98 (s, 1H), 2.01 (s, 3H); LCMS: 459 $[M+H]^+$.

Step 6: 3-(4-Fluorophenyl)-2-(4-iodophenyl)-4-methyl-6-((tetrahydro-2H-pyran-2-yl)oxy)-2H-chromene (13g). Pyridinium *p*-toluenesulfonate (4.50 g, 17.9 mmol) and 3,4-dihydro-2*H*-pyran (16.0 mL, 175 mmol) were added to a mixture of 1-(2,5-dihydroxyphenyl)-2-(4-fluorophenyl)ethanone (41.1 g, 89.7 mmol) and DCM (400 mL) at room temperature. After stirring for 2.5 h, the reaction was diluted with DCM (200 mL), washed (300 mL $NaHCO_3$ and then 300 mL brine), dried ($MgSO_4$), and concentrated under reduced pressure. The residue was purified by silica gel chromatography (0–6% ethyl acetate in hexanes) to give the title compound (37.1 g, 76%) as a pink foam. ^{1}H NMR (400 MHz, DMSO-d_6): δ 7.62 (d, J = 8.3 Hz, 2H), 7.39-7.32 (m, 2H), 7.19 (t, J = 8.9 Hz, 2H), 7.09 (dd, J = 8.4, 1.8 Hz, 2H), 7.02-6.98 (m, 1H), 6.84-6.82 (m, 1H), 6.64 (dd, J = 8.8, 1.4 Hz, 1H), 6.06 (s, 1H), 5.36 (s, 1H), 3.84-3.76 (m, 1H), 3.59-3.50 (m, 1H), 2.04 (s, 3H), 1.92-1.65 (m, 3H), 1.65-1.45 (m, 3H); LCMS: 543 $[M+H]^+$.

3-(3-Hydroxyphenyl)-4-methyl-2-(4-((S)-2-((R)-3-methylpyrrolidin-1-yl)propoxy)phenyl)-2H-chromen-6-ol (14n).

Step 1: (3R)-3-Methyl-1-((2S)-1-(4-(4-methyl-6-((tetrahydro-2H-pyran-2-yl)oxy)-3-(3-((tetrahydro-2H-pyran-2-yl)oxy)phenyl)-2H-chromen-2-yl)phenoxy)propan-2-yl)pyrrolidine. A mixture of **13a** (100.11 g, 160.43 mmol), **7n** (34.43 g, 240.77 mmol), CuI (6.13 g, 32.20 mmol), K_2CO_3 (44.43 g, 321.49 mmol), and butyronitrile (320 mL) was degassed with three vacuum/nitrogen cycles. The reaction mixture was heated at 135 °C (temperature of oil bath) for 4 days, allowed to cool to room temperature, and then diluted with ethyl acetate

(320 mL). The mixture was filtered through a pad of Celite, and the Celite was washed with ethyl acetate (320 mL). The filtrate was washed (2×480 mL water), dried (Na_2SO_4), and concentrated under reduced pressure. The residue was purified by silica gel chromatography (hexanes/ 2% triethylamine in ethyl acetate; 0-75%) to give the desired compound (88.52 g, 86%). ^{1}H NMR (400 MHz, DMSO-d_6): δ 7.25 (t, J = 7.6 Hz, 1H), 7.20 (d, J = 8.6 Hz, 2H), 7.00 (t, J = 2.6 Hz, 1H), 6.95-6.87 (m, 3H), 6.82-6.75 (m, 3H), 6.60 (d, J = 8.6 Hz, 1H), 5.98 (2s, 1H), 5.46-5.36 (m, 1H), 5.35 (m, 1H), 3.97-3.91 (m, 1H), 3.85-3.66 (m, 3H), 3.57-3.45 (m, 2H), 2.84-2.76 (m, 1H), 2.67-2.55 (m, 2H), 2.54-2.46 (m, 1H), 2.07 (m, 5H), 1.50-1.99 (m, 13H), 1.25-1.14 (m, 1H), 1.19 (d, J = 6.4 Hz, 3H), 0.95 (d, J = 6.4 Hz, 3H).

Step 2: 3-(3-Hydroxyphenyl)-4-methyl-2-(4-((S)-2-((R)-3-methylpyrrolidin-1-yl)propoxy)phenyl)-2H-chromen-6-ol (14n). A solution (3*R*)-3-methyl-1-((2*S*)-1-(4-(4-methyl-6-((tetrahydro-2*H*-pyran-2-yl)oxy)-3-(3-((tetrahydro-2*H*-pyran-2-yl)oxy)phenyl)-2*H*-chromen-2-yl)phenoxy)propan-2-yl)pyrrolidine (80.1 g, 125.4 mmol) was stirred in 80% acetic acid/water (1250 mL) at room temperature overnight. The mixture was concentrated under reduced pressure, and the residue was dissolved in ethyl acetate (2000 mL). The organic layer was washed (2×1500 mL saturated $NaHCO_3$), dried (Na_2SO_4), and concentrated under reduced pressure. This crude material was dissolved in ethyl acetate (400 mL) and then stirred until cloudy suspension was obtained without any gummy solid. Hexanes (2400 mL) was added to the suspension, and the mixture was stirred overnight. The resulting precipitate was collected by filtration to give the title compound (48.9 g, 83%) as a tan solid. ^{1}H NMR (400 MHz, DMSO-d_6): δ 9.47 (s, 1H), 8.96 (s, 1H), 7.19 (d, J = 8.7 Hz, 2H), 7.12 (t, J = 7.9 Hz, 1H), 6.79 (d, J = 8.7 Hz, 2H), 6.75-6.72 (m, 1H), 6.70-6.67 (m, 1H), 6.67-6.63 (m, 1H), 6.63-6.61 (m, 1H), 6.50-6.45 (m, 2H), 5.83 (s, 1H), 3.98-3.91 (m, 1H), 3.73-3.66 (m, 1H), 2.84-2.77 (m, 1H), 2.66-2.55 (m,

2H), 2.54-2.47 (m, 1H), 2.13-2.04 (m, 2H), 2.03 (s, 3H), 1.91-1.81 (m, 1H), 1.25-1.15 (m, 1H), 1.05 (d, J = 6.5 Hz, 3H), 0.94 (d, J = 6.4 Hz, 3H); ^{13}C NMR (100 MHz, DMSO-d_6): δ 158.5, 157.1, 151.4, 143.6, 139.6, 132.3, 130.3, 129.4, 129.2, 125.3, 125.2, 119.7, 116.5, 115.9, 115.1, 114.3, 114.1, 110.5, 78.1, 70.8, 58.7, 57.1, 50.4, 32.0, 31.1, 20.3, 15.7, 14.5; HRMS-ESI (m/z): $[M+H]^+$ calcd for $C_{30}H_{33}NO_4$, 472.2488; found, 472.2486.

3-(4-Fluorophenyl)-4-methyl-2-(4-((S)-2-((R)-3-methylpyrrolidin-1-yl)propoxy)phenyl)-2H-chromen-6-ol (15g). The title compound was prepared from **13g** and **7n** following the procedure outlined for **14b**. ^{1}H NMR(400 MHz, DMSO-d_6): δ 8.97 (s, 1H), 7.35-7.29 (m, 2H), 7.21-7.14 (m, 4H), 6.79 (d, J = 8.7 Hz, 2H), 6.76-6.73 (m, 1H), 6.52-6.46 (m, 2H), 5.91 (s, 1H), 3.95 (dd, J = 9.6, 4.3 Hz, 1H), 3.77-3.66 (m, 1H), 2.87-2.75 (m, 1H), 2.69-2.57 (m, 2H), 2.57-2.45 (m, 1H), 2.13-2.03 (m, 2H), 2.01 (s, 3H), 1.92-1.79 (m, 1H), 1.26-1.14 (m, 1H), 1.06 (d, J = 6.4 Hz, 3H), 0.94 (d, J = 6.4 Hz, 3H); ^{13}C NMR (100 MHz, DMSO-d_6): δ 161.1 (d, J = 244.5 Hz), 158.5, 151.5, 143.7, 134.6 (d, J = 3.0 Hz), 131.3, 131.1 (d, J = 8.0 Hz), 129.4, 125.9, 125.0, 116.5, 115.3, 115.1 (d, J = 21.1 Hz), 114.2, 110.6, 78.1, 70.7, 58.7, 57.1, 54.9, 50.5, 32.0, 31.1, 20.2, 15.6, 14.4; HRMS-ESI (m/z): $[M+H]^+$ calcd for $C_{30}H_{32}FNO_3$, 474.2444; found, 474.2439.

Breast Cancer Cell ER-α In Cell Western Assay (ER-α degradation assay). MCF-7 cells were trypsinized and washed twice in phenol red free RPMI containing 5% charcoal dextran stripped FBS with 20 mM HEPES and NEAA and adjusted to a concentration of 200,000 cells per mL with the same medium. Next, 16 μL of the cell suspension (3200 cells) was added to each well of a poly-D-lysine coated 384 well plate, and the cells were incubated at 37 °C over 4 days to allow the cells to adhere and grow. On day 4, a ten point, serial 1:5 dilution of each compound was added to the cells in 16 μL at a final concentration ranging from 10-5M to 5.12 x

10-12M or 10-6M to 5.12 x 10-13M for fulvestrant. At 4 hours post compound addition, the cells were fixed by adding 16 μL of 30% formalin to the 32 μL of cells and compound (10% formalin final concentration) for 20 minutes. Cells were then washed twice with PBS Tween 0.1% and then permeabilized in PBS 0.1% Triton (50μl/well) for additional 15 minutes. The PBS 0.1% triton was decanted, and the cells were washed: LI-COR blocking buffer (50 μL/well) was added, the plate was spun at 3000 rpm, and then the blocking buffer was decanted. Additional LI-COR blocking buffer (50 μL/well) was added, and the cells were incubated overnight at 4 °C. The blocking buffer was decanted, and the cells were incubated overnight at 4 °C with SP1 (Thermo Scientific) anti-ER rabbit monoclonal antibody diluted 1:1000 in LI-COR blocking buffer/0.1% Tween-20. Wells which were treated with blocking buffer with Tween but no antibody were used as a background control. Wells were washed twice with PBS Tween 0.1% to remove free SP1 antibodies, and the cells were incubated at room temp for 60-90 minutes in LI-COR goat anti-rabbit IRDyeTM 800CW (1:1000) and DRAQ5 DNA dye (1:10000 of 5 mM stock solution) diluted in LI-COR blocking buffer containing 0.1% Tween-20 and 0.01% SDS. Cells were then washed with 0.1%Tween-20/PBS three times. Plates were scanned on a LI-COR Odyssey infrared imaging system. Integrated intensities in the 800 nm channel and 700 nm channel were measured to determine levels of ER-α and DNA respectively. Percent ER levels were determined as follows: (Integrated intensity 800 nm sample/integrated intensity 700 nm sample)/ (Integrated intensity 800 nm untreated cells/integrated intensity 700 nm untreated cells) x 100 = %ER-α levels.

Breast Cancer Cell Viability Assay (MCF-7 proliferation assay). MCF-7 cells were adjusted to a concentration of 40,000 cells per mL in RPMI containing 10% FBS and 20 mM HEPES. 16 μL of the cell suspension (640 cells) was added to each well of a 384 well plate, and the cells

were incubated overnight to allow the cells to adhere. The following day a 10 point, serial 1:5 dilution of each compound was added to the cells in 16 µL at a final concentration ranging from 10-0.000005 µM. After 5 days' compound exposure, 16 µL of CellTiter-GLo (Promega) was added to the cells, and the relative luminescence units (RLUs) of each well were determined. CellTiter-Glo added to 32 µL of medium without cells was used to obtain a background value. The percent viability of each sample was determined as follows: (RLU sample-RLU background/RLU untreated cells-RLU background) x 100 = %viability.

Immature Uterine Wet Weight-Antagonist Mode. Female immature CD-IGS rats (21 days old upon arrival) were dosed daily for three days. Vehicle or test compound was administered orally by gavage followed 15 minutes later by an oral dose of 0.1 mg/kg Ethynyl Estradiol. On the fourth day 24 hours after dose, plasma was collected for pharmacokinetic analysis. Immediately following plasma collection, the animals were euthanized and the uterus was removed and weighed.

In-vivo Xenograft Breast Cancer Model; (MCF-7; Tamoxifen-sensitive). Time release pellets containing 0.72 mg 17β-Estradiol were subcutaneously implanted into nu/nu mice. MCF-7 cells were grown in RPMI containing 10% FBS at 5% CO_2, 37 °C. Trypsinized cells were pelleted and re-suspended in 50% RPMI (serum free) and 50% Matrigel at $1X10^7$ cells/mL. MCF-7 cells were subcutaneously injected (100µL/animal) on the right flank 2-3 days post pellet implantation. Tumor volume (length x $width^2/2$) was monitored bi-weekly. When tumors reached an average volume of ~200 mm^3 animals were randomized and treatment was started. Animals were treated with vehicle or compound daily for 4 weeks. Tumor volume and body weight were monitored bi-weekly throughout the study.

In-vivo Xenograft Breast Cancer Model; (Tamoxifen-resistant model). Female nu/nu mice (with supplemental 17β-Estradiol pellets; 0.72mg; 60 day slow release) bearing MCF-7 tumors (mean tumor volume 200mm^3) were treated with Tamoxifen (citrate) by oral gavage. Tumor volume (length x width^2/2) and body weight were monitored twice weekly. Following a significant anti-tumor response in which tumor volume remained static, evident tumor growth was first observed at approximately 100 days of treatment. At 120 days of treatment, tamoxifen dose was increased. Rapidly growing tumors were deemed tamoxifen resistant and selected for in vivo passage into new host animals. Tumor Fragments (~100mm^3/animal) from the tamoxifen resistant tumors were subcutaneously implanted into the right flank of female nu/nu mice (with 17β-Estradiol pellets (0.72mg; 60 day slow release)). Passaged tumors were maintained under constant Tamoxifen selection, and tumor volume (length x width^2/2) was monitored weekly. When tumor volume reached ~150-250 mm^3, animals were randomized into treatment groups (mean tumor volume 200 mm^3) and tamoxifen treatment was terminated. Animals were treated with vehicle or compound daily for 4 weeks. Tumor volume and body weight were monitored twice weekly for the duration of the study.

AUTHOR INFORMATION

Corresponding author:

*Phone: 858-369-7604. E-mail: nsmith@seragonpharm.com.

Notes: The authors declare no competing financial interest

ABBREVIATIONS

AUC, area under the curve; CL, clearance; C_{24}, concentration at 24 hours; Cpd, compound; C_{max}, maximum concentration; C_{min}, minimum concentration; DHP, 3,4-dihydro-2H-pyran; E2, estradiol; EE, ethynyl estradiol; ER, estrogen receptor; ERE, estrogen response element; IPA, 2-propanol; %F, percent oral bioavailability; on, overnight; po, peroral; SAR, structure activity relationship; SERD, selective estrogen receptor degrader; SERM, selective estrogen receptor modulator; $t_{1/2}$, half-life; UWW, uterine wet weight; Vss, volume of distribution at steady state.

ANCILLARY INFORMATION

All animal experiments performed in the manuscript were conducted in compliance with institutional guidelines. A selection of the experimental section is presented below. Please see Supporting Information for full experimental details, 1H NMR, LCMS and HRMS. Molecular Formula Strings have also been submitted.

REFERENCES

1. Nilsson, S.; Gustafsson, J. A., Estrogen receptors: therapies targeted to receptor subtypes. *Clinical pharmacology and therapeutics* **2011,** *89* (1), 44-55.

2. Ariazi, E. A.; Ariazi, J. L.; Cordera, F.; Jordan, V. C., Estrogen receptors as therapeutic targets in breast cancer. *Current topics in medicinal chemistry* **2006,** *6* (3), 181-202.

3. (a) Riggins, R. B.; Schrecengost, R. S.; Guerrero, M. S.; Bouton, A. H., Pathways to tamoxifen resistance. *Cancer letters* **2007,** *256* (1), 1-24. (b) Mills, J. N; Rutkovsky A, C; Giordano A., Mechanisms of resistance in estrogen receptor positive breast cancer: overcoming resistance to tamoxifen/aromatase inhibitors. *Curr Opin Pharmacol.* **2018,** *41*, 59-65. (c) Katzenellenbogen, J. A.; Mayne, C. G.; Katzenellenbogen, B. S.; Greene, G. L.; Chandarlapaty,

S. Structural underpinnings of oestrogen receptor mutations in endocrine therapy resistance. *Nat Rev Cancer.* **2018,** *18(6)*, 377-388.

4. Musgrove, E. A.; Sutherland, R. L., Biological determinants of endocrine resistance in breast cancer. *Nature reviews. Cancer* **2009,** *9* (9), 631-643.

5. (a) Johnston, S. J.; Cheung, K. L., Fulvestrant - a novel endocrine therapy for breast cancer. *Current medicinal chemistry* **2010,** *17* (10), 902-914. Subsequent to the completion of this work, there have been additional reports on SERDs, including: (b) De Savi, C.; Bradbury, R. H.; Rabow, A. A.; Norman, R. A.; de Almeida, C.; Andrews, D. M.; Ballard, P.; Buttar, D.; Callis, R. J.; Currie, G. S.; Curwen, J. O.; Davies, C. D.; Donald, C. S.; Feron, L. J.; Gingell, H.; Glossop, S. C.; Hayter, B. R.; Hussain, S.; Karoutchi, G.; Lamont, S. G.; MacFaul, P.; Moss, T. A.; Pearson, S. E.; Tonge, M.; Walker, G. E.; Weir, H. M.; Wilson, Z. Optimization of a novel binding motif to (E)-3-(3,5-difluoro-4-((1R,3R)-2-(2-fluoro-2-methylpropyl)-3-methyl-2,3,4,9-tetrahydro-1H-pyrido[3,4-b]indol-1-yl)phenyl)acrylic acid (AZD9496), a potent and orally bioavailable selective estrogen receptor downregulator and antagonist. *J. Med. Chem.* **2015**, *58(20)*, 8128-8140. (c) Tria, G. S.; Abrams, T.; Baird, J.; Burks, H. E.; Firestone, B.; Gaither, L. A.; Hamann L. G.; He, G.; Kirby, C. A; Kim, S.; Lombardo, F.; Macchi, K. J.; McDonnell, D. P.; Mishina, Y.; Norris, J. D.; Nunez, J.; Springer, C.; Sun, Y.; Thomsen, N. M.; Wang, C.; Wang, J.; Yu, B.; Tiong-Yip, C. L.; Peukert, S.; Discovery of LSZ102, a potent, orally bioavailable selective estrogen receptor degrader (SERD) for the treatment of estrogen receptor positive breast cancer. *J Med Chem.* **2018**, *61(7)*, 2837-2864. (d) Xiong, R.; Zhao, J.; Gutgesell, L. M.; Wang, Y.; Lee, S.; Karumudi, B.; Zhao, H.; Lu, Y.; Tonetti, D. A.; Thatcher, G. R. Novel selective estrogen receptor downregulators (SERDs) developed against treatment-resistant breast cancer. *J Med Chem.* **2017**, *60(4)*,1325-1342.

6. Lai, A.; Kahraman, M.; Govek, S.; Nagasawa, J.; Bonnefous, C.; Julien, J.; Douglas, K.; Sensintaffar, J.; Lu, N.; Lee, K.-J.; Aparicio, A.; Kaufman, J.; Qian, J.; Shao, G.; Prudente, R.; Joseph, J. D.; Darimont, B.; Brigham, D.; Grillot, K.; Heyman, R.; Rix, P.; Hager, J.; Smith, N. D., Identification of GDC-0810 (ARN-810), an orally bioavailable selective estrogen receptor degrader (SERD) that demonstrates robust activity in tamoxifen-resistant breast cancer xenografts. *Journal of medicinal chemistry* **2015,** *58 (12), 4888–4904.*

7. Gauthier, S.; Caron, B.; Cloutier, J.; Dory, Y. L.; Favre, A.; Larouche, D.; Mailhot, J.; Ouellet, C.; Schwerdtfeger, A.; Leblanc, G.; Martel, C.; Simard, J.; Merand, Y.; Belanger, A.; Labrie, C.; Labrie, F., (S)-(+)-4-[7-(2,2-dimethyl-1-oxopropoxy)-4-methyl-2-[4-[2-(1-piperidinyl)-ethoxy] phenyl]-2H-1-benzopyran-3-yl]-phenyl 2,2-dimethylpropanoate (EM-800): a highly potent, specific, and orally active nonsteroidal antiestrogen. *Journal of medicinal chemistry* **1997,** *40* (14), 2117-2122.

8. Veeneman, G. H., Non-steroidal subtype selective estrogens. *Current medicinal chemistry* **2005,** *12* (9), 1077-1136.

9. (a) Chandrasekaran, A.; McKeand, W. E.; Sullivan, P.; DeMaio, W.; Stoltz, R.; Scatina, J., Metabolic disposition of [14C]bazedoxifene in healthy postmenopausal women. *Drug metabolism and disposition: the biological fate of chemicals* **2009,** *37* (6), 1219-1225; (b) Snyder, K. R.; Sparano, N.; Malinowski, J. M., Raloxifene hydrochloride. *American journal of health-system pharmacy : AJHP : official journal of the American Society of Health-System Pharmacists* **2000,** *57* (18), 1669-1675; quiz 1676-8.

10. Kim, S.; Wu, J.; Chen, H. Y.; Birzin, E. T.; Chan, W.; Yang, Y. T.; Colwell, L.; Li, S.; Dahllund, J.; DiNinno, F.; Rohrer, S. P.; Schaeffer, J. M.; Hammond, M. L., Estrogen receptor

ligands. Part 4: The SAR of the syn-dihydrobenzoxathiin SERAMs. *Bioorganic & medicinal chemistry letters* **2004,** *14* (11), 2741-2745.

11. Tan, Q.; Blizzard, T. A.; Morgan, J. D., 2nd; Birzin, E. T.; Chan, W.; Yang, Y. T.; Pai, L. Y.; Hayes, E. C.; DaSilva, C. A.; Warrier, S.; Yudkovitz, J.; Wilkinson, H. A.; Sharma, N.; Fitzgerald, P. M.; Li, S.; Colwell, L.; Fisher, J. E.; Adamski, S.; Reszka, A. A.; Kimmel, D.; DiNinno, F.; Rohrer, S. P.; Freedman, L. P.; Schaeffer, J. M.; Hammond, M. L., Estrogen receptor ligands. Part 10: Chromanes: old scaffolds for new SERAMs. *Bioorganic & medicinal chemistry letters* **2005,** *15* (6), 1675-1681.

12. Littke, A.; Soumeillant, M.; Iii, R. F.; Cherney, R. J.; Tarby, C. M.; Kiau, S., Mild and general methods for the palladium-catalyzed cyanation of aryl and heteroaryl chlorides. *Organic letters* **2007,** *9* (9), 1711-1714.

13. Zhu, W.; Ma, D., Synthesis of aryl sulfones via L-proline-promoted CuI-catalyzed coupling reaction of aryl halides with sulfinic acid salts. *The Journal of organic chemistry* **2005,** *70* (7), 2696-2700.

14. Marsaud, V.; Gougelet, A.; Maillard, S.; Renoir, J. M., Various phosphorylation pathways, depending on agonist and antagonist binding to endogenous estrogen receptor alpha (ERalpha), differentially affect ERalpha extractability, proteasome-mediated stability, and transcriptional activity in human breast cancer cells. *Molecular endocrinology* **2003,** *17* (10), 2013-2027.

15. Plasma AUC is for the mixture of the two diastereoeisomers from the chromene core. It is formally possible that the diastereoisomeric pairs of compounds could be metabolized differently in-vivo. However it was found that **14na** and **14nb** had very similar exposure. For example,

following a 30 mg/Kg po dose: For **14na** (n = 4): Cmax = 0.40 ug/mL, AUC = 3.10 ug.h/mL. For **14nb** (n = 1): Cmax = 0.44 ug/mL, AUC = 3.44 ug.h/mL.

16. The ability to reduce uterine weight below that of the vehicle in immature rats may reflect a low level of basal ER activity in the rat uterus of vehicle treated animals, or that although immature, the rats still have a low level of circulating estrogen.

17. Lee, J. S.; Ettinger, B.; Stanczyk, F. Z.; Vittinghoff, E.; Hanes, V.; Cauley, J. A.; Chandler, W.; Settlage, J.; Beattie, M. S.; Folkerd, E.; Dowsett, M.; Grady, D.; Cummings, S. R., Comparison of methods to measure low serum estradiol levels in postmenopausal women. *The Journal of clinical endocrinology and metabolism* **2006,** *91* (10), 3791-3797.

TABLE OF CONTENTS GRAPHIC

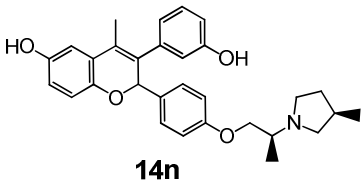
HO
OH
O
O
N

14n

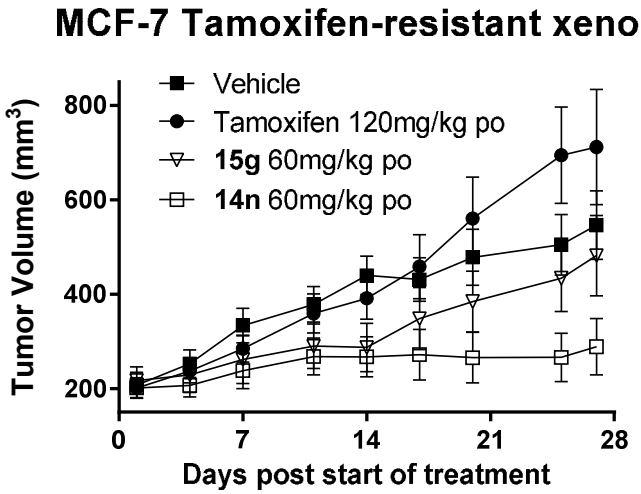
MCF-7 Tamoxifen-resistant xenograft
Vehicle
Tamoxifen 120mg/kg po
15g 60mg/kg po
14n 60mg/kg po
Tumor Volume (mm3)
800
600
400
200
0
7
14
21
28
Days post start of treatment